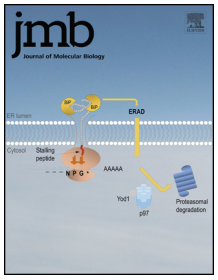

A Molecular Target for an Alcohol Chain-Length Cutoff

Hae-Won Chung[1,2,†], E. Nicholas Petersen[1,2,†], Cerrone Cabanos[1,2], Keith R. Murphy[2,3,4], Mahmud Arif Pavel[1,2], Andrew S. Hansen[5], William W. Ja[2,3] and Scott B. Hansen[1,2]

*1 - **Department of Molecular Medicine,** The Scripps Research Institute, Jupiter, FL 33458, USA*
*2 - **Department of Neuroscience,** The Scripps Research Institute, Jupiter, FL 33458, USA*
*3 - **Center on Aging,** The Scripps Research Institute, Jupiter, FL 33458, USA*
*4 - **Program in Integrative Biology and Neuroscience,** Florida Atlantic University, Jupiter, FL 33458, USA*
*5 - **HBBiotech,** BioInnovations Gateway, Salt Lake City, UT 84115, USA*

***Correspondence to Scott B. Hansen:** Department of Molecular Medicine, The Scripps Research Institute, Jupiter, FL 33458, USA. shansen@scripps.edu*
https://doi.org/10.1016/j.jmb.2018.11.028
Edited by Daniel L. Minor

Abstract

Despite the widespread consumption of ethanol, mechanisms underlying its anesthetic effects remain uncertain. *n*-Alcohols induce anesthesia up to a specific chain length and then lose potency—an observation known as the "chain-length cutoff effect." This cutoff effect is thought to be mediated by alcohol binding sites on proteins such as ion channels, but where these sites are for long-chain alcohols and how they mediate a cutoff remain poorly defined. In animals, the enzyme phospholipase D (PLD) has been shown to generate alcohol metabolites (e.g., phosphatidylethanol) with a cutoff, but no phenotype has been shown connecting PLD to an anesthetic effect. Here we show loss of PLD blocks ethanol-mediated hyperactivity in *Drosophila melanogaster* (fruit fly), demonstrating that PLD mediates behavioral responses to alcohol *in vivo*. Furthermore, the metabolite phosphatidylethanol directly competes for the endogenous PLD product phosphatidic acid at lipid-binding sites within potassium channels [e.g., TWIK-related K^+ channel type 1 (K2P2.1, TREK-1)]. This gives rise to a PLD-dependent cutoff in TREK-1. We propose an alcohol pathway where PLD produces lipid-alcohol metabolites that bind to and regulate downstream effector molecules including lipid-regulated potassium channels.

Introduction

The molecular mechanism of ethanol intoxication is historically linked to an anesthetic effect. In the late 1800s, Meyer and Overton showed that *n*-alcohols increase in potency based on their hydrophobicity [1]. However, in a homologous series with increasing length, the increase in potency plateaued at 11 carbons and then became inactive at 14 carbons. For example, in tadpoles, the alcohol dodecanol (C12) is a potent anesthetic (i.e., effective at low concentration), but tetradecanol (C14) is not [2]. Over the ensuing 50 years, a debate arose as to molecular determinants of this cutoff [3,4]. Enantiomers of alcohols were not selective [5] suggesting a membrane site of action, but the effects of long-chain alcohols on bulk membranes alone appeared to be insufficient for anesthesia [6]. We asked if an intermediary metabolite may contribute to the anesthetic effect of long-chain alcohols on ion channels.

Phospholipase D2 (PLD2) is a membrane-associated protein that, in the presence of alcohol, generates the unnatural lipid phosphatidylalcohol (POH) in a process known as transphosphatidylation [7] (Supplementary Fig. 1b). Ethanol transphosphatidylation is significantly elevated in alcoholics and individuals with a history of alcohol abuse suggesting an *in vivo* role for phosphatidylethanol (PEtOH) [8]. Like ethanol, long-chain *n*-alcohols are substrates for PLD2 transphosphatidylation and exhibit

a chain-length cutoff around eight carbons [9,10]. But the question remains, do PLD2 metabolites contribute to alcohol's effect on ion channel and animal behavior?

Ion channels are major effectors of ethanol intoxication [11] and potential downstream targets of phosphatidylalcohols. Anionic signaling lipids, in particular PLD-derived phosphatidic acid (PA), and phosphatidylinositol (4,5)-bisphosphate (PIP_2), regulate many ion channels [12–14] often at specific lipid sites within the channels [12,15–17] (Supplementary Fig. 1a). We hypothesized that PLD-derived ethanol metabolites could bind to the lipid regulatory sites of some ion channels and compete for endogenous PA or PIP_2 regulators. Many channels exhibit a cutoff with a length of 8–11 carbons (Supplementary Table S1). Molecular sites of ethanol have been characterized in detail for select channels [11], but the molecular basis for long-chain alcohol cutoff sites on channels is poorly defined. If PLD-derived POH binds to any of these lipid regulatory sites, this would represent a new form of regulation distinct from the usual receptor–alcohol interaction and link alcohol metabolites directly to ion channel function.

Here we show PLD2-dependent metabolites bind to the lipid regulatory sites of two-pore domain potassium (K2P) channels and regulate function in a chain-length dependent manner. Furthermore, loss of PLD in flies blocks an ethanol-induced hyperactive response, confirming an *in vivo* role for PLD in ethanol sensitivity.

Results

In vivo role of PLD in alcohol intoxication

Despite PLD's well-known role in generating ethanol metabolites, the *in vivo* relevance of the metabolites to ethanol intoxication has yet to be established. If PLD ethanol metabolism is relevant to the physiological effects of alcohol intoxication, we would expect the loss of PLD to also result in a loss of an alcohol phenotype. Like mammals, flies have a hyperactive response to ethanol prior to sedation [18] making flies a suitable model for genetic interrogation. Knockout of the *pld* gene (PLD^{null}) in *Drosophila melanogaster* (fruit flies) was previously shown to eliminate transphosphatidylation in the animal [19]. Unlike mammals, *D. melanogaster* only have one isoform of PLD, making this a complete loss of all PLD lipase activity. We obtained the PLD^{null} flies previously shown to be devoid of transphosphatidylation activity [19].

To test a PLD-dependent transphosphatidylation response to ethanol, we monitored a hyperactive response after ethanol consumption in PLD^{null} flies. Animals were simultaneously monitored for activity and feeding with ethanol using video tracking [20,21] (Fig. 1a). PLD^{null} mutants robustly blocked the response of ethanol when compared to genetically matched wild-type controls (Fig. 1b). To ensure that this effect was a neuronal-specific effect, we used the GAL4/UAS system to knock down the *pld* gene by expressing an RNAi construct under the control of a pan-neuronal GAL4 driver ($nSyb^{GAL4}$). PLD KD also robustly blocked the ethanol hyperactivity response in flies compared to control (Fig. 1d). The behavior was significant for two independent RNAi lines tested ($p = 0.018$ and 0.023; Fig. 1d and Supplementary Fig. S2a). The lack of ethanol response in PLD KD flies was not due to feeding since all groups exhibited similar avoidance as expected for short term exposure [22] (Fig. 1c, e, and Supplementary Fig. S2b). KD flies were hyperactive under starvation conditions, confirming that the lack of effect seen during ethanol administration was not due to an activity ceiling caused by the PLD KD. We also confirmed that the KD animals are capable of normal hyperactivity by moving the flies to agar without food and monitoring activity for 24 h (Supplementary Fig. S2c).

The strong alcohol phenotype in PLD mutant flies suggests that a product of PLD is involved in alcohol intoxication. We considered both POH accumulation and PA depletion as likely downstream perturbations accounting for the alcohol phenotype. First, we investigated PA depletion in the presence of 0.3% ethanol (a clinical concentration) using partially purified mammalian PLD2 enzyme. Thin layer chromatography analysis of PLD2 lipid products showed PLD2 continues to robustly produce PA in the presence of ethanol (Supplementary Fig. S1d), suggesting that ethanol does not block PA production, but rather PEtOH is an added metabolite. We confirmed this result in the brains of intoxicated mice using quantitative whole-cell shotgun lipidomics. Among the 13 PA species identified, none showed any significant change in concentration in the presence of ethanol (Supplementary Fig. S3). PLD2 can also produce phosphatidylglycerol (PG) in the presence of glycerol [23]. All species of PG levels also remained unchanged in the presence of ethanol.

Unlike PA, which is rapidly metabolized, PEtOH is a long-lived metabolite and accumulates in plasma membrane of cells and blood after alcohol consumption, most notably in the brain [24] reaching levels up to 1%–2% of the lipid membrane [25]. PEtOH is structurally similar to PA, differing by only two carbons, suggesting that the metabolites could compete at PA binding sites (Supplementary Fig. S1c and Supplementary Discussion). This led us to consider PA-regulated ion channels, in particular channels activated by PA in sensory and excitatory neurons, as possible targets of PEtOH inhibition. K^+ channels reduce neuronal firing; hence, we expect channels inhibited by PEtOH to contribute to a hyperactive response.

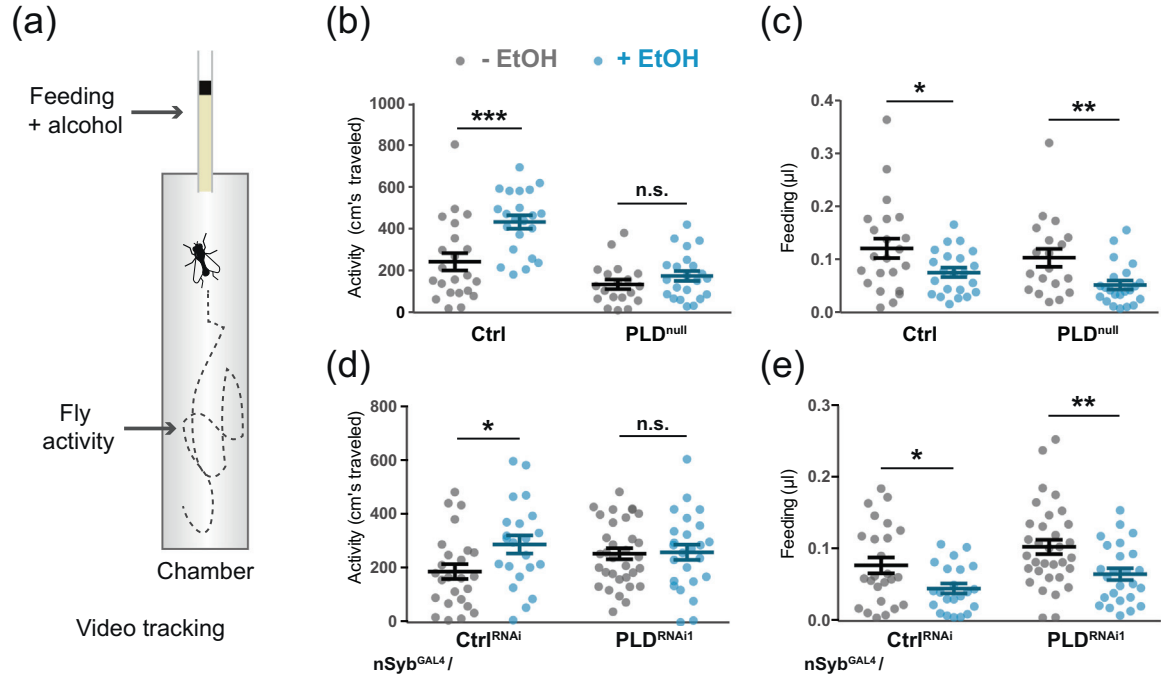

Fig. 1. PLD inhibition in *D. melanogaster* blocks alcohol hyperactivity. (a) Flies fed 30% ethanol were monitored for activity and feeding by video tracking. (b) Complete knockout of PLD (PLD3.1) blocked ethanol-induced hyperactive response ($p = 0.23$, n = 19–22) compared to control flies (w1118; $p = 0.0007$, n = 22). (c) Short-term exposure to ethanol decreased feeding similarly in control ($p = 0.03$) and knockout ($p = 0.007$) flies (n = 19–22). (d) Pan-neuronal expression of PLD RNAi, under an nSyb^{Gal4} driver, (independent lines RNAi1 and RNAi2; see Supplementary Fig. S5 for RNAi2 data) showed the same effect in hyperactive response ($p = 0.018$ and 0.023) but not control vector (Ctrl). (e) Decreased feeding ($p = 0.02$) was similarly observed in ctrl and PLD RNAi expressing flies (**$p < 0.001$ and *$p < 0.05$, two-tailed Student's *t* test; RNAi1, n = 22–32; RNAi2, n = 9–16).

PEtOH inhibition of K^+ channels

TWIK-related K^+ channel type 1 (K2P2.1, TREK-1) and TWIK-related arachidonic acid-activated K^+ channel (K2P4.1, TRAAK) are dimeric K2P channels that are activated by PA and contribute to resting membrane potential of sensory nerves and cardiac tissue [16,26–28]. PLD localizes with and activates TREK-1 through production of PA [29] and PG [16,30]. Alcohol inhibits TREK-1 in a PLD2-dependent manner [29], but whether the metabolite can directly antagonize the channel has not been tested. To directly test the metabolite for a potential role in K2P channel function, we employed lipid-binding and functionality assays with purified protein *in vitro* [16] (Fig. 2a–c).

We found that PEtOH directly competes with lipid agonist sites in both TRAAK and TREK-1 channels (Fig. 2b–c). The channels were purified to homogeneity in detergent micelles and directly assayed using a PIP_2 competition assay for detecting lipid binding to potassium channels [16] (Supplementary Fig. S4a and Fig. 2a). PEtOH bound TRAAK with a K_d of 106 ± 30. TREK-1 with a K_d of 123 ± 37 µM compared to 15.7 ± 6 µM for PA and 177 ± 30 µM for PG [16]. These K_d values agree with the established mechanism that localized high levels of anionic lipid activate the channel [29].

Most PA channels also bind PIP_2 and have opposing effects [15,16], suggesting that each site can bind both antagonizing and agonizing lipids. PEtOH could also compete with PIP_2 sites in PIP_2-regulated channels. Kir2.1 and Kir2.2 are tetrameric PIP_2-gated channels that are antagonized by PA—PA competes out agonizing PIP_2 [15,31]. Like TREK-1, Kir channels contribute to the resting membrane potential [32] and ethanol can inhibit their function [33,34]. As expected, we found that similar to K2P channels, PEtOH directly competes with PIP_2 binding to Kir2.1 and Kir2.2 (K_d of 70.0 and 131 µM, respectively; see Fig. 2d and Supplementary Fig. S4d–e). These relative affinities suggest that PEtOH could shift the channel toward a closed state by increasing the overall concentration of antagonizing lipid (e.g., mix with antagonizing PIP_2).

Next, we tested PEtOH's ability to inhibit TREK-1 and TRAAK conductance using an ion flux assay (Fig. 3a–c and Supplementary Fig. S4b). First we reconstituted purified TREK-1 channels into PC liposomes with either 15% PEtOH or control 15%

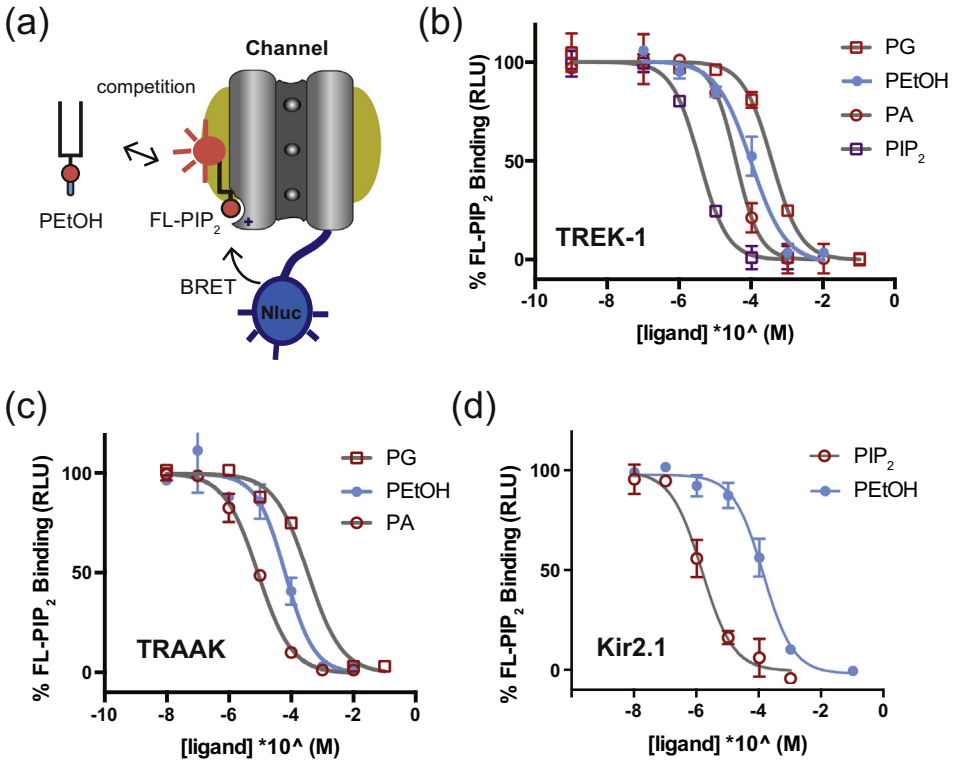

Fig. 2. PEtOH directly binds to K+ channels. Soluble fluorescent PIP_2 (FL-PIP_2) competition assays. (a) Cartoon showing experimental design. Purified TREK-1 channel (gray) in a detergent micelle (yellow), with a genetically encoded nano-luciferase (Nluc) tag, binds FL-PIP_2 (red lipid). Bound FL-PIP_2 produces a bioluminescence resonance energy transfer (BRET) signal. (b–d) PEtOH (blue) dose dependently competes with fluorescent probe. Competition curves for endogenous agonists (red) and antagonists (purple) are plotted for the respective channels. (a) PEtOH bound TREK-1with a K_d of 123 ± 37 μM. (b) TRAAK with a K_d of 106 ± 30 μM. (c) Kir2.1 with a K_d of 70.0 ± 28 μM (average ± SEM, n = 3).

PG alone and assayed the ability of the channel to release potassium [16,35]. We previously showed that 15% PG optimally agonizes TREK-1 [16]. TREK-1 in liposomes with 15% PEtOH released very little potassium compared to robust flux by 15% PG (Fig. 3a). This is significant since PG has a lower affinity than PEtOH (Fig. 2b). Next, we tested functional competition of PEtOH in the presence of PG to determine if PEtOH had any effect on channel conductance. The addition of 15% PEtOH to liposomes with PG (10%) antagonized both TREK-1 and TRAAK ion flux (Fig. 3b–c).

Unlike PEtOH, un-metabolized ethanol had no effect on TREK-1 ion conductance when reconstituted into purified PC/PG lipid vesicles (Fig. 3a, d, purple trace). To further confirm that ethanol is not an allosteric antagonist, we tested ethanol binding to TREK-1 and TRAAK in our lipid-binding assay [16]. Consistent with the ion flux data, ethanol had no effect on PIP_2 binding to TREK-1 or TRAAK (Fig. 3e), while norfluoxetine (NFX), a TREK-1-specific allosteric antagonist [36], completely blocked PIP_2 binding ($p < 0.0001$) to TREK-1. Similarly, free ethanol had no detectable allosteric effect on PIP_2 binding to Kir2.2 (Supplementary Fig. S4f). These results suggest that the lipid metabolites rather than the free alcohol antagonize the channels (Fig. 3f).

PLD2 chain-length cutoff in TREK-1 channels

Previous studies showed that PLD2 produces metabolites with a chain-length cutoff near eight carbons [9,10]. We confirmed the ability of PLD2 to transphosphatidylate long-chain alcohols in the presence of a series of homologous *n*-alcohols of increasing chain length from methanol (C1) to hexadecanol (C16) by following the reaction using a fluorescent version of PC (Supplementary Fig. S5a). We overexpressed the mammalian enzyme in HEK293 cells (mPLD) and partially purified the enzyme in a microsomal fraction. Consistent with the previous studies, we found PLD2 transphosphatidylates alcohols of increasing chain length up to octanol (C8), but alcohols longer than octanol had no transphosphatidylated product (Fig. 4a–b, see zoomed view with a red line after the final observed product). Because PLD2 is an enzyme and any product that is formed can accumulate, we defined the

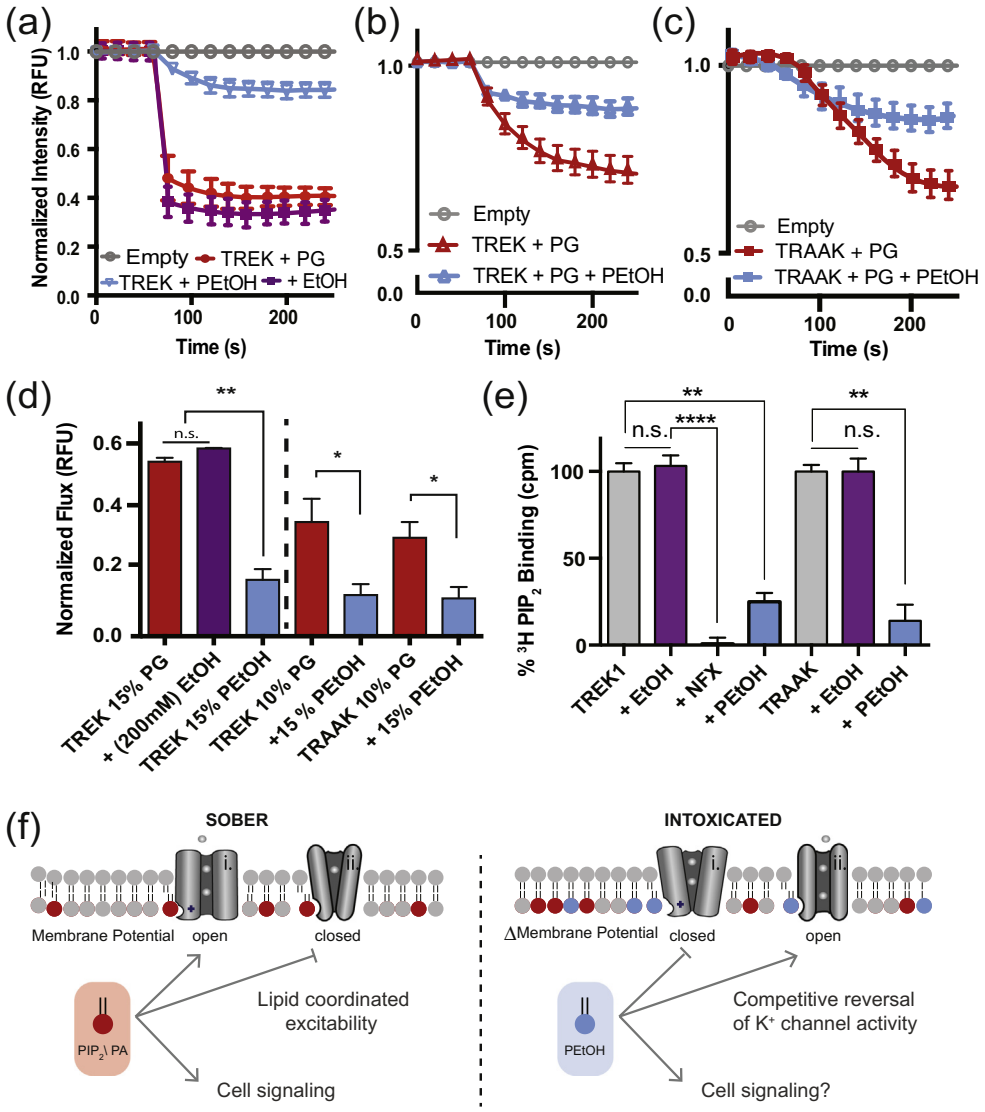

Fig. 3. PEtOH antagonizes K+ channel ion flux. (a–d) K^+ channels were reconstituted into synthetic POPC lipid vesicles with PG (lipid agonist) or PEtOH or both and assayed by an ion flux assay. Efflux of potassium causes fluorescence quenching. (a) TREK-1 with 15% PG robustly causes ion flux (quenching) but 15% PEtOH does not. (b–c) Ion flux assays with mixtures of PG and PEtOH. PEtOH (15%, blue) competes out 10% PG to antagonize TREK-1 (b) and TRAAK (c) channels relative to PG alone (10%, red). (d) Quantification of panels a–c at time 250 s. Free ethanol has no effect on flux (purple; $^*p < 0.05$ and $^{**}p < 0.01$, two-tailed Student's *t* test; n = 5–11). (e) Nor does free ethanol (purple) have an effect on PIP_2 binding to detergent purified TREK and TRAAK measured in a scintillation proximity assay. In contrasts, the allosteric antagonist norfluoxetine robustly inhibits PIP_2 binding ($^{**}p < 0.01$ and $^{****}p < 0.0001$, two-tailed Student's *t* test; n = 2–4). (f) Proposed model for a PEtOH induced intoxication. (Left) A PIP_2- and PA-driven cooperation of channels and transporters sets the excitability of the cell membrane. PA activates some channels (i., e.g., K2P channels), closes others (ii., eg. Kv; see also Discussion) and effects other cell signals (see Supplementary Fig. 1a). (Right) In the presence of ethanol, PA concentrations remain constant, but PLD-generated PEtOH (blue lipids) accumulates and directly competes with PA and PIP_2 in the lipid regulatory sites, leading to a change in membrane polarization and nerve excitability.

cutoff after the last visible product. To identify the longest possible metabolite, we used the highest concentration permitted by solubility in detergent and incubated 3 h. The presence of detergent in our assay buffer permitted very high concentrations of long-chain alcohols (see Methods). The high concentration of alcohol did not alter enzyme activity as PLD2 catalyzed robust transphosphatidylation in 1 M methanol and ethanol (Fig. 4b). We also tested a smaller substrate, lysophosphatidylcholine (LPC), which lacks an acyl chain compared to PC (Fig. 4c). We found that the chain-length cutoff was three carbons

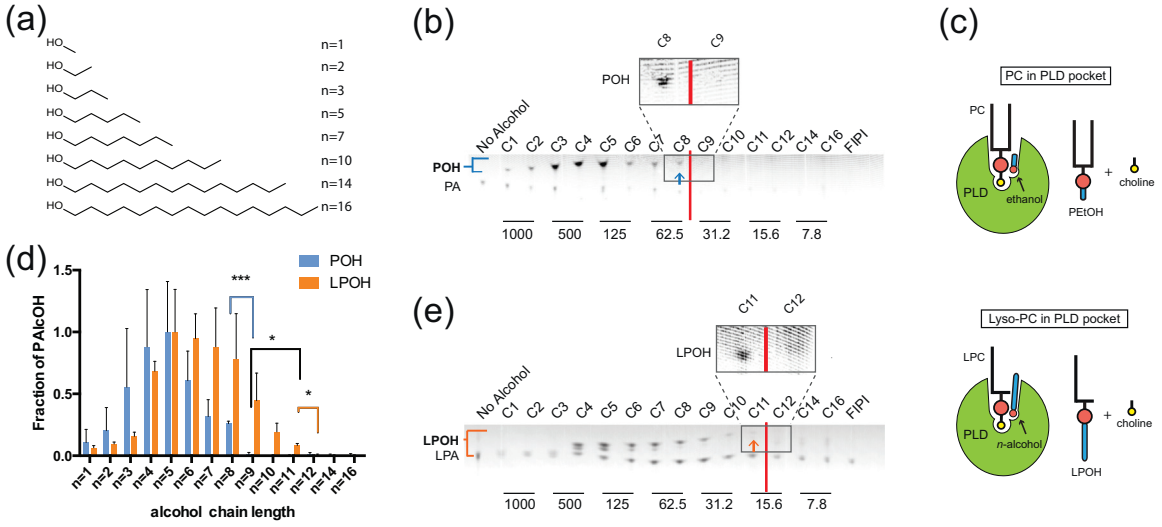

Fig. 4. *n*-Alcohol chain-length cutoff in PLD. (a) Diagram of the primary alcohols used in the following experiments. (b) TLC analysis of mouse PLD exposed to a series of *n*-alcohol (n = 1–16) with PC substrate. The carbon chain length is indicated above each respective lane, and the concentration alcohol used in the reaction (mM) is indicated below. Alcohols of longer chain length migrate faster, and a blue bar indicates the range of POH products. A blue arrow indicates the last transphosphatidylated product, and a red line indicates the chain length cutoff (see also zoomed inset). (c) Proposed model for PLD transphosphatidylation comparing the substrates PC (top) and LPC (bottom) in a catalytic pocket. PC, with two acyl chains, yields a smaller binding surface for *n*-alcohols compared to LPC, which has only one acyl chain. (d) Quantification of TLC analysis with both full (blue) and lyso (orange) PC. Significant changes occur in the amount of transphosphatidylation as noted above (n = 3; $*p < 0.05$ and $**p < 0.01$ with Student's *t* test). (e) Representative image of lysoPC transphosphatidylation with a noted cutoff between 11 and 12 carbons.

longer (after C11) when LPC was the substrate compared to PC (Fig. 4d–e).

Since the microsomal fractions containing mPLD could also contain other contaminating lipases, we confirmed the cutoff in purified cabbage PLD (cPLD). Under identical experimental conditions and lipids, cPLD exhibited a cutoff two carbons longer compared to mPLD2 (C10 *versus* C8; Supplementary Fig. S5b–c and Fig. 4b, respectively; see also Supplementary Discussion). Similarly, the products from LPC were three carbons longer with cPLD enzyme compared to mPLD2 (C14 *versus* C11; see Figs. S5b–c, and 4e, respectively). The potency of alcohols was dose dependent and increased with chain length (Supplementary Fig. S5d–f).

If a PLD transphosphatidylation product is responsible for TREK-1 inhibition, then the channel should have a chain-length cutoff dependent on PLD enzymatic activity. Using the cutoff determined with PLD2 as a prediction for TREK-1 inhibition and using whole cell patch clamp as a measurement, we found that octanol (eight carbons) and ethanol robustly inhibit TREK-1 currents in HEK293 cells expressing TREK-1 channels (Fig. 5a–b and Supplementary Fig. S6). The inhibition was found to be PLD dependent. We then tested dodecanol—as predicted by the PLD cutoff, inhibition decreased to near control levels. Some residual (though statistically insignificant) inhibition appears to remain, which may indicate a contribution from a PLD-independent pathway.

Discussion

Our combined data show that PLD2 transphosphatidylation mediates a chain-length cutoff in TREK-1 channels. Therefore, PLD2 contains the binding site (and thus the location of the cutoff) for long-chain alcohols and not the ion channel (Supplemental Fig. S7). The role of PLD2 for the sedative effects of alcohols in animals remains to be determined. Our behavior assays were limited by the ability to administer alcohols through feeding and thus could not induce sedation. The length of the cutoff in PLD does roughly correlate with the phenotypic cutoff, but direct experimentation is needed to show that ethanol and long-chain alcohols are working the same in animals as they do with TREK-1. Hence the conclusion of this paper is limited to illustrating an indirect cutoff in the channel, despite PLD2 having a significant role in ethanol hyperactivity.

Our indirect mechanism of long-chain alcohol sensitivity on TREK-1 channels does not preclude direct binding sites in other channels. For example, a computational docking study found a putative direct-

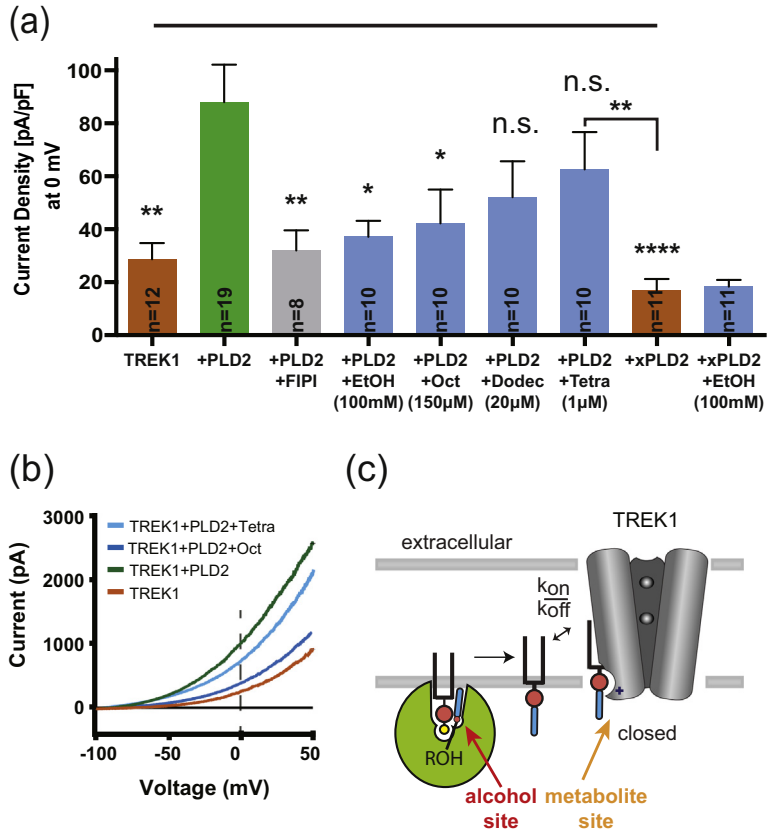

Fig. 5. PLD-dependent chain-length cutoff in TREK-1. PLD2 binds to the C-terminus of TREK and activates the channel [29]. (a) The summary of hTREK-1 current density at 0 mV showing the alcohol chain-length dependence. Alcohols up to octanol show clear inhibition; the effect diminishes significantly with alcohol chain lengths of 12 and 14 carbons (****$p < 0.0001$, **$p < 0.01$, and *$p < 0.05$ with Mann–Whitney 95% confidence level). PLD2 K758R mutation (xPLD2) renders PLD2 catalytically dead. Alcohol concentrations used are noted below each bar. (b) Overexpression of PLD2 enhances TREK-1 up to 3-fold (green trace). Treatment (1 h) with long-chain alcohol octanol (blue trace) blocked this effect, but the long-chain alcohol tetradecanol had very little effect (cyan trace). (c) Cartoon of showing a PLD-dependent cutoff in TREK-1. The cutoff in TREK-1 is a two-step process that involves both PLD2 and TREK-1. The alcohol site in PLD where the cutoff is proposed is labeled in red, while the metabolite binding site on TREK-1 is noted in orange. PLD2 and POHs are labeled as in Fig. 3. TREK-1 is shown as gray cylinders in a closed state with a POH bound. Gray bars delineate the plasma membrane with the bottom facing the cytosol.

binding site for long-chain alcohols in BK channels [37]. Ethanol and long-chain alcohols appeared to bind to the same site. Ethanol sites in G-protein-coupled inward-rectifying potassium channel (GIRK) and pentameric *Gloeobacter* ligand-gated ion channel (GLIC) are well characterized by X-ray crystallography [33,38] and ethanol directly agonizes GIRK in a purified system [39], but little structural information is known about how long-chain alcohols regulate these systems.

A single channel like TREK is not likely to produce the complex behavior effects of alcohol intoxication, but a single lipid acting on multiple channels could. Channels like TREK-1 that are agonized by PA and directly inhibited by PIP_2 [16] are likely the most affected since PEtOH and PIP_2 would combine to antagonize PA, and PA is in relatively low concentrations in the cell. PIP_2 can also indirectly activate TREK-1 through PIP_2 agonism of PLD2 [16], making PIP_2 regulation complicated [40]. However, this occurs at low concentration of PIP_2 [40], so we still expect PEtOH to compete and inhibit the channel. Many channels could be indirectly agonized or antagonized by POH, and each target will need to be considered independently to test the role of PLD2 in a cutoff.

In sensory nerves, K2Ps hyperpolarize the membrane, inhibiting the nerve [41,42]. Hence, inhibiting K2Ps leads to increased excitability. In theory, PEtOH could also mediate the paradoxical sedation of ethanol by antagonizing a separate class of ion channels at high concentration. For example, PEtOH binding to Kv channels increases the channel's gating voltage by 40 mV, near resting membrane potentials [43]. This facilitates Kv opening (opposite the effect of K2Ps) in resting cells and would maintain hyperpolarization, a sedative effect. In both cases, PEtOH competes with the endogenous lipid, exerting an effect opposite the endogenous function (see Fig. 3f). The differential effects of PEtOH on K^+ channels could contribute to the complex excitatory and inhibitory states of ethanol on animals (including humans and flies) [18].

Ethanol is typically considered a general anesthetic, yet ethanol has the opposite effect of volatile anesthetics on TREK-1—volatile anesthetics activate TREK-1 [44]. We have shown that volatile anesthetics activate TREK-1 by robustly activating PLD2 [45], a result that nicely explains the atypical response of ethanol to this anesthetic sensitive channel, further suggesting the mechanism for volatile anesthetics

could related to ethanol through PLD for some channels.

In conclusion, we show that PEtOH is an important metabolite for understanding the molecular processes of alcohol in ion channel function, and we show that PLD2 is critical for dictating the sensitivity of flies to ethanol. Since anionic lipids can centrally regulate the activity of channels involved in cell excitability and inebriation, targeting lipid-signaling pathways may be useful in treating the effects of alcohol in addition to other related neurological diseases.

Methods

Reagents

Bacterial (*Streptomyces chromofuscus*), peanut, and cabbage PLD was purchased from Enzo and Sigma-Aldrich, respectively. Amplex Red 10-acetyl-3,7-dihydroxyphenoxazine was from Cayman Chemical), horseradish peroxidase was from VWR (Radnor, PA), and choline oxidase was from (VWR). All lipids including 1,2-dioctanoyl-sn-glycero-3-phosphocholine (C8-PC), 1-palmitoyl-2-(dipyrromethene boron difluoride) undecanoyl-*sn*-glycero-3-phosphocholine (TopFluorPC), 1-(dipyrromethene boron difluoride) undecanoyl-2-hydroxy-*sn*-glycero-3-phosphocholine (TopFluorLPC), 1-palmitoyl-2-oleoyl-*sn*-glycero-3-phospho-(1′-*rac*-glycerol; POPG), 1,2-dioleoyl-*sn*-glycero-3-phosphocholine (DOPC or 18:1 PC), 1-palmitoyl-2-oleoyl-*sn*-glycero-3-phosphoethanol (POPEtOH), and 1,2-dioleoyl-*sn*-glycero-3-phosphoethanol (DOPEtOH) were purchased from Avanti Polar Lipids (Alabaster, AL) in chloroform at stock concentrations of 10 or 25 mg/mL except C8-PC and TopFluor lipids, which were purchased as powder. Carbonyl cyanide *m*-chlorophenyl hydrazine (CCCP) was from Tocris Bioscience and made at a stock concentration of 1 mM in ethanol. Valinomycin was also purchased from Tocris Bioscience and made at a stock concentration of 200 μM in ethanol. The detergent *n*-dodecyl-β-D-maltoside (DDM) was purchased from Anatrace (D310S) and made at 200 mM. ACMA (9-amino-6-chloro-2-methoxyacridine) was purchased from Life Technologies and made at a stock concentration of 2 mM in ethanol.

Drosophila culture and lines

Flies were raised on 6-oz bottles containing a standard cornmeal–sucrose–yeast medium consisting of (weight/volume) 5.8% cornmeal, 3.1% active dry yeast, 0.7% agar, 1.2% sucrose, and (volume/volume) 1% propionic acid and 0.22% Tegosept (weight/volume, pre-dissolved in ethanol). Males were collected 0–2 days following eclosion using CO_2 anesthesia and kept on standard diet at ~10 flies per vial (polystyrene, 25 × 95 mm). Flies were maintained and tested in a temperature- and humidity-controlled incubator at 25 °C and ~60% relative humidity with a 12:12-h light/dark cycle. Experiments were performed using 4- to 9-day-old males [20,21]. pld^{RNAi2} (TRiP, RRID:BDSC_32839) was obtained from the Bloomington Stock Center. pld^{RNAi1} (VDRC, v106137) was obtained from the Vienna *Drosophila* Resource Center. $dPLD^{3.1}$ knockout flies were a gift from Padinjat Raghu.

Diets and starve–refeed paradigm

Liquid diets were made by combining 2.5% sucrose and 2.5% Bacto yeast extract (weight/volume) in 70 mL ddH_2O and gently heating until homogenous, followed by filtration (0.2-μm cellulose acetate syringe filter; VWR). Fifteen milliliters of either 100% ethanol or nanopure water was added to 35 mL of liquid diet and vortexed. The reagents were obtained from Fisher Scientific (Waltham, MA) or VWR.

Behavioral recording was performed using the ARC, as described previously [20]. Prior to recording, animals were placed in the ARC for 16 h with an empty capillary for starvation. The capillaries were switched at ZT 0 with capillaries containing the control or ethanol diet followed by 30 min of behavioral recording. Animals that did not consume food in that period were excluded from analysis.

Shotgun lipidomics

Tissue preparation (HEK and mouse brain)

HEK cell was grown in 10 cm plate at 80% confluency and treated with 0.3% ethanol (no addition for control) in growth media. After 1-h incubation at 37 °C, the cultured cells were washed with ice-cold PBS and scraped into 15-mL Falcon tube and pelleted by centrifugation at 1000*g*. The pellet was kept at −80 °C until further analysis. For mouse brain, four mice were injected with 2.4 g/kg of ethanol twice with 20-min interval. After the second injection (~45 min total), the mice were euthanized under CO_2 (control mice were euthanized the same way without ethanol treatment) and brains were extracted and flash frozen with liquid nitrogen. Brains from the four mice were collected and milled in liquid nitrogen. The milled powder was kept at −80 °C until further analysis.

Lipid extraction

HEK cells or mouse brain samples were added 300 μL of 10 times diluted PBS in an Eppendorf tube and were homogenized for 1 min by using a disposable soft tissue homogenizer. An aliquot of 25 μL was pipetted to determine the protein content (BCA protein assay kit; Thermo Scientific, Rockford,

IL). The rest of homogenate was accurately transferred into a disposable glass culture test tube, and a mixture of lipid internal standards was added prior to lipid extraction for quantification of all reported lipid species. Lipid extraction was performed by using a modified Bligh and Dyer procedure as described previously [46]. Each lipid extract was resuspended into a volume of 500 µL of chloroform/methanol (1:1, v/v) per mg of protein and flushed with nitrogen, capped, and stored at −20 °C for lipid analysis.

Mass spectrometric analysis

For ESI direct infusion analysis, lipid extract was further diluted to a final concentration of ~500 fmol/µL, and the mass spectrometric analysis was performed on a QqQ mass spectrometer (Thermo TSQ VANTAGE, San Jose, CA) equipped with an automated nanospray device (TriVersa NanoMate; Advion Bioscience Ltd., Ithaca, NY).

TREK-1 lipid-binding assays

Cloning, expression, and purification of TREK-1

A gene corresponding to human TREK-1 (GI:14589851) amino acids 1–411 was codon-optimized for eukaryotic expression, synthesized (Genewiz, Inc.), amplified by PCR the truncated form (amino acids 1–321, adapted from previously reported stable truncated form of zebrafish TREK-1 [35] [47], and ligated into the EcoRI/XhoI restriction sites of a modified pPICZ-B vector (Invitrogen). The resulting protein is linked at the C-terminus to fluorescent protein with a 10xHis tag *via* a short linker (SNS) followed by a PreScission protease cleavage site (LEVLFQ/GP). The resulting vector was linearized with PmeI and transformed into *Pichia pastoris* strain SMD1163 by electroporation. Transformants were selected by plating on YPDS plates with 1 mg/mL zeocin. Large-scale expression was performed in 2.8-L baffled flasks. Overnight cultures of cells grown in YPD with 0.4 mg/mL zeocin were added to 1 L buffered minimal-glycerol media, and grown overnight at 30 °C, 250 rpm to an OD600 ~16. Cells were then harvested at 1500*g*, resuspended in 1 L buffered minimal-methanol media, and incubation temperature was reduced to 25 °C. Induction was maintained by addition of 0.5% methanol every 12 h. Expression was continued for ~48–60 h. Cells were pelleted, frozen in liquid nitrogen, and stored at −80 °C.

Cells were disrupted by milling (Retsch model MM400) 5 times for 2.5 min at 25 Hz. All subsequent purification steps were carried out at 4 °C. Cell powder was added to lysis buffer [50 mM Tris (pH 8.0), 150 mM KCl, 60 mM DDM (Affymetrix), 0.1 mg/mL DNAse 1, 0.1 µg/mL pepstatin, 1 µg/mL leupeptin, 1 µg/mL aprotinin, 0.1 mg/mL soy trypsin inhibitor, 1 mM benzamidine, and 0.1 mg/mL AEBSF, with 1 mM phenylmethysulfonyl fluoride added immediately before use] at a ratio of 1 g cell pellet/4 mL lysis buffer. Membranes were extracted for 4 h with stirring followed by centrifugation at 35,000*g* for 45 min. The supernatant was then applied to a manually packed Cobalt resin (Clontech) gravity-flow column, then serially washed and eluted in IMAC buffer [50 mM Tris (pH 8.0), 150 mM KCl, 4 mM DDM] with 30 and 300 mM imidazole (pH 8.0). Eluted protein was then concentrated (50 kDa MWCO) and applied to a Superdex 200 column (GE Healthcare) equilibrated in SEC buffer [20 mM Tris (pH 8.0), 150 mM KCl, 1 mM EDTA, 2 mM DDM].

Scintillation proximity assay (SPA)

Scintillation proximity assay was carried out in 0.6-mL centrifuge tubes with a 50-µL total reaction volume consisting of 25 nM (100 nM binding sites) of purified TREK-1, 0.6 mg/mL of PVT (polyvinyl toluene) anti-mouse antibody bead (PerkinElmer), 0.1 mg/mL of anti-His tag mAb (R&D Systems), 200 nM of inositol-2-^{3}H(*N*)]-phosphatidylinositol-4,5-bisphosphate (^{3}H-PIP$_2$; PerkinElmer), and increasing concentration of nonradioactive 16:0 PEtOH or 1,2-dipalmitoyl-*sn*-glycero-3-phosphoethanol (1 µM to 1 mM PEtOH; Avanti Polar Lipids) in SEC buffer with 7 mM DDM final concentration. Nonradioactive PEtOH was first incubated for ~2 h prior to adding the radioactive PIP$_2$ and further incubated for 18–28 h or until an equilibrium in signal is reached. Light emitted brought about by binding of ^{3}H-PIP$_2$ to TREK1-Ab-bead complex and competition with PEtOH was measured using LS6500 Multi-Purpose Scintillation Counter (Beckman Coulter). The FL-PIP$_2$ affinities of 1.3, 1.8, 0.22, and 0.12 µM were calculated from saturation curves of TREK-1, TRAAK, Kir2.1, and Kir2.2, respectively (data not shown), and used to calculate the K_d values of PEtOH.

BRET

The BRET binding assay was performed here as done previously [16]. Briefly, the bioluminescence resonance energy transfer was done in a 384-well plate, with each well having a total of 50-µL total reaction volume consisting of ~1 nM purified ion channel tagged with Nluc, 500 nM of BODIPY-TMR phosphatidylinositol 4,5-bisphosphate (FL-PIP$_2$; Echelon Biosciences), various concentrations of competing ligand and 1:2000 furimazine (NanoGlo, Promega), the substrate for Nluc, in SEC buffer with 7 mM DDM final concentration as described previously [16]. BRET signal brought about by the binding of FL-PIP$_2$ to TREK-1-Nluc and competition with a ligand was calculated by subtracting signal from Nluc only control and measured using Tecan Spark

20 M plate reader set for dual-emission detection (540 nM for Nluc and 574 nM for FL-PIP_2) and automatic BRET ratio calculation.

Ion channel flux assay

Proteoliposome formation was followed according to previously published literature [48]. A total of 3 μmol lipids were mixed together in the desired molar ratio (85:15) in a glass round bottom tube and dried with a continuous stream of argon gas until chloroform was no longer visible. The dried lipids were then washed once with pentane and then dried again with argon. The tube was then wrapped in aluminum foil and placed in a vacuum desiccator overnight to remove any further traces of organic solvent. The next morning, dried lipids were rehydrated with 1 mL buffer [150 mM KCl, 20 mM Hepes (pH 7.4)] for 30 min to form a 3 mM solution, and vigorous vortexing was then applied for 10 min to form multilamellar vesicles. The lipid solution was then sonicated in a bath sonicator (Avanti) to reach optical clarity, typically within 5–10 min depending on the PC chain length, leading to formation of unilamellar vesicles. Liposomes were then destabilized with DDM, and the concentration added (3 mM) was based on the necessary amount to form saturated lipid-detergent vesicles [48]. A three-hour time period was then observed to allow for DDM to equilibrate in the membranes [49]. Then, the solution was evenly divided into two 0.6-mL microtubes, one to be used for the empty reconstitution control and the other for zTREK reconstitution. Next, empty reconstitution control solution [150 mM KCl, 20 mM Hepes (pH 7.4), 2 mM DDM] or GFP-zTREK was added to the solution at a 1:100 (mass/mass) protein/lipid ratio [48] and gently rocked for 1 h at room temperature. The solution was then transferred to a 5-mL Eppendorf tube and topped to 3 mL with the rehydration solution. Detergent was then removed using BioBeads SM-2 polystyrene beads (Bio-Rad, washed three times with methanol, three times with water, three times with rehydration buffer, 20 min each wash). Approximately 100 mg of beads, which is beyond the adsorptive capacity for the amount of DDM present in the tubes [49], was added to the solution and gently rocked for 1.5 h, previously shown to be enough time for detergent removal and preventing the formation of multilamellar vesicles [49]. The solution was then transferred to a 3.2-mL centrifuge tube (Beckman, 362305) and centrifuged at 250,000*g* for 45 min at 20 °C using a TLA110 rotor in an Optima XP ultracentrifuge (Beckman Coulter). The supernatant was removed, and proteoliposomes were resuspended in 150 μL rehydration buffer. Following brief sonication, reconstitution was checked by measuring GFP fluorescence on a Tecan Spark 20M plate reader. Flux assays were performed immediately after. Proteoliposomes were then flash-frozen and stored at −80 °C.

Flux measurements were performed similarly as previously published [35]. Briefly, 5 μL of sonicated proteoliposomes was added to 195 μL of flux assay buffer [150 mM NaCl, 20 mM Hepes (pH 7.4), 2 μM ACMA] in duplicates in a black 96-well plate (Costar 3915). A protocol was set up on a Tecan Spark 20 M to initially read the fluorescence every 20 s for 1 min as a baseline. The temperature inside the plate reader was set at 25 °C. Then, using the protonophore CCCP (1 μM final concentration), we collapsed the electrical potential and initiated potassium flux. Fluorescence was read every 20 s for 7 min. Next, the potassium-selective ionophore valinomycin (20 nM final concentration) was added to terminate the chemical gradient, and fluorescence was read every 20 s for 5 min. An average of the duplicates was taken, and then the data were normalized similar to that published in Su et al. [50]. Briefly, at each time point $(F - F_{start})/(F_{start} - F_{end})$ was calculated, where F is the fluorescent value at that time, F_{start} is the average of the first four initial readings before the addition of CCCP, and F_{end} is the final fluorescent value after 5 min of valinomycin. Next, control proteoliposome flux was normalized to 1 throughout CCCP, and the TREK flux was normalized to the control accordingly. In flux assay figures, addition of CCCP occurs at $t = 80$ s and ends at $t = 500$ s before valinomycin was added.

PLD product release assay (purified protein and cultured cells)

Cell culture

Tetracycline-inducible CHO stable cells expressing mPLD2 [51] were grown in F-12 (Ham) medium including 10% tetracycline-free FBS, 100 U/mL penicillin, 100 μg/mL streptomycin, 10 μg/mL blasticidin, and 300 μg/mL Zeocin. In order to induce PLD expression, 1 μg/mL tetracycline was added 1 day before experiments.

mPLD2 expressed CHO cells were seeded into 96-well culture plate (~5×10^4 cells per well) and incubated at 37 °C overnight to let the cells were fully attached and stabilized to the plate. The cells were washed twice with PBS and incubate with 50 μL PBS containing 17.5 mM glucose until the PLD assay reaction starts. The PLD reaction was started as described in PLD *in vitro* assay session.

Assay measurements

PLD activity was measured by enzyme-coupled assay using 10-acetyl-3, 7-dihydroxyphenoxazine (Amplex Red reagent) with slight modifications [52]. Fifty microliters of PLD-containing samples in reaction

buffer [50 mM Hepes, 5 mM $CaCl_2$ (pH 8.0)] was aliquoted into 96-well plate. Each reaction was initiated by adding 50 μL of working solution containing 100 μM Amplex Red, 2 U/mL horseradish peroxidase, 0.2 U/mL choline oxidase, and 60 μM 1,2-dioctanoyl-sn-glycero-3-phosphocholine (C8 PC) with the indicated amount of anesthetic compounds to make the final concentration of each component to be twofold lower. Fluorescence was kinetically measured for 1 h at 37 °C with microplate reader (Tecan Infinite 200 Pro) at excitation and emission wavelengths of 530 and 585 nm, respectively.

PLD transphosphatidylation assay (thin-layer chromatography)

PLD transphosphatidylation assay was carried out as described previously with slight modifications [10] (2). The substrate 1-palmitoyl-2-(dipyrromethene-boron difluoride) undecanoyl-*sn*-glycero-3-phosphocholine (TopFluorPC) or 1-(dipyrromethene-boron difluoride) undecanoyl-2-hydroxy-*sn*-glycero-3-phosphocholine (TopFluor LPC) was sonicated in 66 mM Mes (pH 6.0) buffer containing 0.5 mM octylglucoside, 400 mM NaCl, and the test alcohol as indicated. The mPLD-CHO cells were cultured in 10-cm plate and induced with tetracycline. The following day, mPLD2 was activated by incubating with 100 nM phorbol 12-myristate 13-acetate (PMA) for 10 min at 37 °C. After washing cells with cold PBS, cells were scraped and lysed in the lysis buffer [20 mM Hepes (pH 7.5), 80 mM β-glycerophosphate, 10 mM EGTA, 2 mM EDTA, and 5 mM DTT]. Sample was sonicated and spun at 10,000*g* for 20 min at 4 °C. The pellet was resuspended in reaction buffer [50 mM Hepes, 5 mM $CaCl_2$ (pH 8.0)]. The PLD transphosphatidylation was initiated by the addition of 10 μL of cabbage PLD (200 U/mL) or mPLD2-CHO membrane resuspension (10-cm plate cells in 40 μL buffer) to the 10 μL substrate solution. The reactions were incubated for 3 h at 30 °C. The samples were applied to a silica gel HL plate (Analtech), and the plate was developed with chloroform/methanol/water/acetic acid (25:7:1:1) solvent. Image was taken using Typhoon imager.

The concentration of long-chain alcohols in 0.5 mM octylglucoside detergent was selected based on solubility. Solubility was determined by visual inspection with no visible partitioning or precipitation. The cutoff in PLD2 is defined as the longest alcohol where a product was visible. Since PLD2 is an enzyme and the product accumulates, the rate of catalysis is not likely the limiting factor.

TREK-1 whole-cell recordings

Reagents 0.6% ethanol (104 mM, KOPTEC) was directly added to the external solution. 1-octanol (Sigma), 1-dodecanol (Acros Organics), 1-tetradecanol (Acros Organics), and FIPI (Calbiochem) were made as stock solutions in DMSO, then added into external solution with the sonication using Avanti Sonicator (model no. G112SP1T_B) in the final concentrations of 150, 20, 1, and 1 μM, respectively. The residual DMSO amount in the bath was maintained $<0.05\%$. Quinidine (200 μM) was directly added into the external solution with sonication. All the salts for internal/external solutions were purchased from either Sigma or Fisher Scientific.

Cell culture and gene expression

HEK293t cells were maintained in the solution consisting of the DMEM (Corning Cellgro) culture media, 10% FBS, 100 units/mL penicillin, and 100 μg/mL streptomycin. Cells were plated on poly-D-lysine-coated 12-mm microscope cover glass ~12, ~36, or ~60 h before transfection in low confluence (5%, 2.5%, or 1.25%). Genes for target proteins were transiently co-transfected in HEK293t cells with X-tremeGENE 9 DNA transfection agent (Roche Diagnostics). Full-length human TREK1 with C-terminus GFP tag in pCEH vector was a gift from Dr. Stephen Long. Mouse PLD2 constructs without GFP tag in pCGN vector were gifts from Dr. Michael Frohman. Both functional PLD2 and inactive mutant PLD2-K758R [53], single mutation form of mPLD2, were used together blindly to test PLD2 effect on TREK1. TREK1 and PLD2 were co-transfected 1 (0.5 μg)/4(2 μg) ratio [29], otherwise a total 1 μg of DNA was used in transfection.

Electrophysiology

The transfected HEK293t cells were used in 18–24 h (TREK1 expression) or 24–30 h (TREK1 + PLD2 co-expression) after transfection. Standard whole-cell patch-clamp procedure for TREK1 was performed according to previous studies [29] [47]. Currents were recorded at room temperature with Axopatch 200B amplifier and Digidata 1440A (Molecular Devices) on a Windows 7-based personal computer. Borosilicate glass electrode pipettes (B150-86-10; Sutter Instrument) were pulled with the Flaming/Brown micropipette puller (Model P-1000; Sutter instrument) resulting in 4–7 MΩ resistances with the internal solution (in mM): 140 KCl, 3 $MgCl_2$, 5 EGTA, and 10 Hepes (pH 7.4; adjusted with KOH). External solution consists of the following (in mM): 145 NaCl, 4 KCl, 2 $CaCl_2$, 1 $MgCl_2$, and 10 Hepes (pH 7.4; adjusted with NaOH). TEA (10 mM), which has been known to be insensitive to TREK1 current [54], was added into both internal/external solutions to block the endogenous potassium channels in HEK293 cells [55]. Patch electrodes were wrapped with parafilm to reduce capacitance, and series resistance was compensated by ~70% (both prediction and correction). Currents measured using Clampex 10.3 (Molecular Devices)

were filtered at 2 kHz, sampled at 10 kHz, and stored on a hard disk for later analysis. Data were analyzed offline by a homemade procedure using IgorPro 6.34A (WaveMetrics). Currents were elicited by a biphasic step voltage command (at −10 and − 100 mV from V_{hold} = −60 mV) and ramp voltage commands (short ramp = −120 to −10 mV in 440 ms, and long ramp = −100 to +50 mV in 1 s) in the absence and presence of quinidine (200 μM), which was used as a known TREK1 blocker [56]. The subtracted 200 μM quinidine-sensitive currents from the long ramp were used to obtain the current density at 0 mV. Drugs including 1-octanol, 1-dodecanol, and 1-tetradecanol, with final concentrations of 150, 20, 1 μM, respectively, were applied using a gravity-driven bath application setup. For alcohol experiments, both protracted treatment (>1 h of incubation) plus bath application of the same drug were performed. Mann–Whitney test was done to assess statistical significance using Prism6 (GraphPad software), and outliers were eliminated using a built-in function in Prism with Q = 1%.

Acknowledgments

We thank Michael Frohman from Stony Brook for the mouse PLD and mutant PLD cDNA; Steven Long from Memorial Sloan Kettering for human TREK-1-GFP; Guangwei Du from UT Health Science Center for PLD expressing cells; Rod Mackinnon from the Rockefeller University for PICZ vectors; Padinjat Raghu for the PLD mutant *Drosophila*; Andrew S. Hansen for PLD experiments, multiple aspects of experimental design, and discussion; Yul Young Park for the electrophysiology experimentation; Arman Nayebosadri for flux experiments; and Nick Franks from Imperial College London for helpful discussion of the manuscript. This work was supported by a Director's New Innovator Award to S.B.H. (1DP2NS087943-01) and an RO1 to W.W.J (R01AG045036) from the National Institutes of Health and a graduate fellowship from the Joseph B. Scheller & Rita P. Scheller Charitable Foundation to E.N.P.

Author Contributions: H.C. E.N.P, and A.S.H developed methodology for PLD studies. H.C. investigated PLD chain length cutoff and provided formal analysis. E.N.P performed data collection and formal analysis for flux assays and PIP_2/ion channel competition studies with supervision from C.C. and E.N.P collected data and designed methodology for fly study with supervision from K.M. and W.W.J. M.A.P collected data and analyzed super resolution imaging and some ion flux experiments. S.B.H. and H.C. wrote the original draft with review and editing from E.N.P and W.W.J.

Competing Financial Interests: The authors declare no competing financial interests.

Appendix A. Supplementary data

Supplementary data to this article can be found online at https://doi.org/10.1016/j.jmb.2018.11.028.

Received 7 September 2018;
Received in revised form 30 November 2018;
Accepted 30 November 2018
Available online 5 December 2018

Keywords:
lipids;
metabolite;
ethanol;
phospholipase;
ion channel

†These authors contributed equally.

Abbreviations used:
PLD, phospholipase D; POH, phosphatidylalcohol; PEtOH, phosphatidylethanol; PA, phosphatidic acid; PIP_2, phosphatidylinositol (4,5)-bisphosphate; PG, phosphatidylglycerol; LPC, lysophosphatidylcholine; K2P, two-pore-domain potassium channel; KD, knock down; BRET, bioluminescence resonance energy transfer.

References

[1] N.P. Franks, W.R. Lieb, Molecular and cellular mechanisms of general anaesthesia, Nature 367 (1994) 607–614, https://doi.org/10.1038/367607a0.
[2] M.J. Pringle, K.B. Brown, K.W. Miller, Can the lipid theories of anesthesia account for the cutoff in anesthetic potency in homologous series of alcohols? Mol. Pharmacol. 19 (1981) 49–55.
[3] N.P. Franks, W.R. Lieb, Mapping of general anaesthetic target sites provides a molecular basis for cutoff effects, Nature 316 (1985) 349–351.
[4] J.K. Alifimoff, L.L. Firestone, K.W. Miller, Anaesthetic potencies of primary alkanols: implications for the molecular dimensions of the anaesthetic site, Br. J. Pharmacol. 96 (1989) 9–16, https://doi.org/10.1111/j.1476-5381.1989.tb11777.x.
[5] J.K. Alifimoff, L.L. Firestone, K.W. Miller, Anesthetic potencies of secondary alcohol enantiomers, Anesthesiology 66 (1987) 55–59, https://doi.org/10.1167/8.5.1.
[6] R.W. Peoples, L. Chaoying, F.F. Weight, Lipid vs protein theories of alcohol action in the nervous system, Annu. Rev. Pharmacol. Toxicol. 36 (1996) 185–201, https://doi.org/10.1146/annurev.pa.36.040196.001153.
[7] M. Kobayashi, J.N. Kanfer, Phosphatidylethanol formation via transphosphatidylation by rat brain synaptosomal phospholipase D, J. Neurochem. 48 (1987) 1597–1603, https://doi.org/10.1111/j.1471-4159.1987.tb05707.x.
[8] G.C. Mueller, M.F. Fleming, M.A. Lemahieu, G.S. Lybrand, K.J. Barry, Synthesis of phosphatidylethanol—a potential marker for adult males at risk for alcoholism, Proc. Natl. Acad. Sci. U. S. A. 85 (1988) 9778–9782.

[9] L. Seidler, M. Kaszkin, V. Kinzel, Primary alcohols and phosphatidylcholine metabolism in rat brain synaptosomal membranes via phospholipase D, Pharmacol. Toxicol. 78 (1996) 249–253.
[10] K.M. Ella, K.E. Meier, A. Kumar, Y. Zhang, G.P. Meier, Utilization of alcohols by plant and mammalian phospholipase D, Biochem. Mol. Biol. Int. 41 (1997) 715–724.
[11] R.J. Howard, P.A. Slesinger, D.L. Davies, J. Das, J.R. Trudell, R.A. Harris, Alcohol-binding sites in distinct brain proteins: the quest for atomic level resolution, Alcohol. Clin. Exp. Res. 35 (2011) 1561–1573, https://doi.org/10.1111/j.1530-0277.2011.01502.x.
[12] S.B. Hansen, Lipid agonism: the PIP2 paradigm of ligand-gated ion channels, Biochim. Biophys. Acta 1851 (2015) 620–628, https://doi.org/10.1016/j.bbalip.2015.01.011.
[13] B. Hille, E.J. Dickson, M. Kruse, O. Vivas, B. Suh, Phosphoinositides regulate ion channels, Biochim. Biophys. Acta (2014) https://doi.org/10.1016/j.bbalip.2014.09.010.
[14] J.F. Hancock, PA promoted to manager, Nat. Cell Biol. 9 (2007) 615–617, https://doi.org/10.1038/ncb0607-615.
[15] S.B. Hansen, X. Tao, R. MacKinnon, Structural basis of PIP2 activation of the classical inward rectifier K+ channel Kir2.2, Nature 477 (2011) 495–498, https://doi.org/10.1038/nature10370.
[16] C. Cabanos, M. Wang, X. Han, S.B. Hansen, A soluble fluorescent binding assay reveals PIP2 antagonism of TREK-1 channels, Cell Rep. 20 (2017) 1287–1294, https://doi.org/10.1016/j.celrep.2017.07.034.
[17] P.L. Yeagle, Non-covalent binding of membrane lipids to membrane proteins, Biochim. Biophys. Acta Biomembr. 1838 (2014) 1548–1559, https://doi.org/10.1016/j.bbamem.2013.11.009.
[18] F.W. Wolf, A.R. Rodan, L.T.-Y. Tsai, U. Heberlein, High-resolution analysis of ethanol-induced locomotor stimulation in *Drosophila*, J. Neurosci. 22 (2002) 11035–11044 (doi:22/24/11035 [pii]).
[19] R. Thakur, A. Panda, E. Coessens, N. Raj, S. Yadav, S. Balakrishnan, et al., Phospholipase D activity couples plasma membrane endocytosis with retromer dependent recycling, elife 5 (2016) 1–23, https://doi.org/10.7554/eLife.18515.
[20] K.R. Murphy, S.A. Deshpande, M.E. Yurgel, J.P. Quinn, J.L. Weissbach, A.C. Keene, et al., Postprandial sleep mechanics in *Drosophila*, elife 5 (2016) 1–19, https://doi.org/10.7554/eLife.19334.
[21] K.R. Murphy, J.H. Park, R. Huber, W.W. Ja, Simultaneous measurement of sleep and feeding in individual *Drosophila*, Nat. Protoc. 12 (2017) 2355–2366, https://doi.org/10.1038/nprot.2017.096.
[22] K.R. Kaun, R. Azanchi, Z. Maung, J. Hirsh, U. Heberlein, A *Drosophila* model for alcohol reward, Nat. Neurosci. 14 (2011) 612–619, https://doi.org/10.1038/nn.2805.
[23] R.M. Dawson, The formation of phosphatidylglycerol and other phospholipids by the transferase activity of phospholipase D, Biochem. J. 102 (1967) 205–210, https://doi.org/10.1042/bj1020205.
[24] A. Brühl, A. Faldum, K. Löffelholz, Degradation of phosphatidylethanol counteracts the apparent phospholipase D-mediated formation in heart and other organs, Biochim. Biophys. Acta Mol. Cell Biol. Lipids 1633 (2003) 84–89, https://doi.org/10.1016/S1388-1981(03)00090-8.
[25] A. Nalesso, G. Viel, G. Cecchetto, D. Mioni, G. Pessa, D. Favretto, et al., Quantitative profiling of phosphatidylethanol molecular species in human blood by liquid chromatography high resolution mass spectrometry, J. Chromatogr. A 1218 (2011) 8423–8431, https://doi.org/10.1016/j.chroma.2011.09.068.
[26] M. Fink, F. Lesage, F. Duprat, C. Heurteaux, R. Reyes, M. Fosset, et al., A neuronal two P domain K+ channel stimulated by arachidonic acid and polyunsaturated fatty acids, EMBO J. 17 (1998) 3297–3308, https://doi.org/10.1093/emboj/17.12.3297.
[27] P. Enyedi, G. Czirják, Molecular background of leak K+ currents: two-pore domain potassium channels, Physiol. Rev. 90 (2010) 559–605, https://doi.org/10.1152/physrev.00029.2009.
[28] M. Fink, F. Duprat, F. Lesage, R. Reyes, G. Romey, C. Heurteaux, et al., Cloning, functional expression and brain localization of a novel unconventional outward rectifier K+ channel, EMBO J. 15 (1996) 6854–6862.
[29] Y. Comoglio, J. Levitz, M.A. Kienzler, F. Lesage, E.Y. Isacoff, G. Sandoz, Phospholipase D2 specifically regulates TREK potassium channels via direct interaction and local production of phosphatidic acid, Proc. Natl. Acad. Sci. U. S. A. 111 (2014) 13547–13552, https://doi.org/10.1073/pnas.1407160111.
[30] S.F. Yang, S. Freer, A.A. Benson, L. Jolla, Transphosphatidylation by phospholipase D, J. Biol. Chem. 242 (1967) 477–484.
[31] S.-J. Lee, S. Wang, W. Borschel, S. Heyman, J. Gyore, C.G. Nichols, Secondary anionic phospholipid binding site and gating mechanism in Kir2.1 inward rectifier channels, Nat. Commun. 4 (2013), 2786. https://doi.org/10.1038/ncomms3786.
[32] H. Hibino, A. Inanobe, K. Furutani, S. Murakami, I.A.N. Findlay, Y. Kurachi, Inwardly rectifying potassium channels: their structure, function, and physiological roles, Physiol. Rev. 90 (2010) 291–366, https://doi.org/10.1152/physrev.00021.2009.
[33] P. Aryal, H. Dvir, S. Choe, P.A. Slesinger, A discrete alcohol pocket involved in GIRK channel activation, Nat. Neurosci. 12 (2009) 988–995, https://doi.org/10.1038/nn.2358.
[34] M. Bebarova, P. Matejovic, M. Pasek, M. Simurdova, J. Simurda, Dual effect of ethanol on inward rectifier potassium current IK1 in rat ventricular myocytes, J. Physiol. Pharmacol. 65 (2014) 497–509.
[35] S.G. Brohawn, J. del Marmol, R. MacKinnon, J. del Mármol, Crystal structure of the human K2P TRAAK, a lipid- and mechano-sensitive K+ ion channel, Science (80-) 335 (2012) 436–441, https://doi.org/10.1126/science.1213808.
[36] Y.Y. Dong, A.C.W. Pike, A. Mackenzie, C. Mcclenaghan, P. Aryal, L. Dong, et al., K2P channel gating mechanisms revealed by structures of TREK-2 and a complex with Prozac, Science 347 (2015) 1256–1259, https://doi.org/10.1126/science.1261512.
[37] A.N. Bukiya, G. Kuntamallappanavar, J. Edwards, A.K. Singh, B. Shivakumar, A.M. Dopico, An alcohol-sensing site in the calcium- and voltage-gated, large conductance potassium (BK) channel, Proc. Natl. Acad. Sci. 111 (2014) 9313–9318, https://doi.org/10.1073/pnas.1317363111.
[38] L. Sauguet, R.J. Howard, L. Malherbe, U.S. Lee, P.J. Corringer, R. Adron Harris, et al., Structural basis for potentiation by alcohols and anaesthetics in a ligand-gated ion channel, Nat. Commun. 4 (2013) 1–10, https://doi.org/10.1038/ncomms2682.
[39] I.W. Glaaser, P.A. Slesinger, Dual activation of neuronal G protein-gated inwardly rectifying potassium (GIRK) channels by cholesterol and alcohol, Sci. Rep. 7 (2017) 1–11, https://doi.org/10.1038/s41598-017-04681-x.
[40] J. Chemin, A.J. Patel, F. Duprat, F. Sachs, M. Lazdunski, E. Honore, Up- and down-regulation of the mechano-gated K2P channel TREK-1 by PIP2 and other membrane phospholipids,

Pflugers Arch. - Eur. J. Physiol. 455 (2007) 97–103, https://doi.org/10.1007/s00424-007-0250-2.
[41] A. Alloui, K. Zimmermann, J. Mamet, F. Duprat, J. Noël, J. Chemin, et al., TREK-1, a K+ channel involved in polymodal pain perception, EMBO J. 25 (2006) 2368–2376, https://doi.org/10.1038/sj.emboj.7601116.
[42] F. Maingret, I. Lauritzen, A.J. Patel, C. Heurteaux, R. Reyes, F. Lesage, et al., TREK-1 is a heat-activated background K(+) channel, EMBO J. 19 (2000) 2483–2491, https://doi.org/10.1093/emboj/19.11.2483.
[43] R.K. Hite, J.A. Butterwick, R. MacKinnon, Phosphatidic acid modulation of Kv channel voltage sensor function, elife 3 (2014) https://doi.org/10.7554/eLife.04366.
[44] A.J. Patel, E. Honoré, F. Lesage, M. Fink, G. Romey, M. Lazdunski, Inhalational anesthetics activate two-pore-domain background K+ channels, Nat. Neurosci. 2 (1999) 422–426, https://doi.org/10.1038/8084.
[45] M.A. Pavel, E.N. Petersen, R.A. Lerner, S.B. Hansen, Studies on the mechanism of general anesthesia, BioRxiv (2018) https://doi.org/10.1101/313973.